AIAA JOURNAL
Vol. 40, No. 7, July 2002

Mixing Process in a Lobed Jet Flow

Hui Hu,* Tetsuo Saga,† Toshio Kobayashi,‡ and Nobuyuki Taniguchi§
University of Tokyo, Tokyo 153-8505, Japan

A high-resolution stereoscopic particle image velocimetry (PIV) system was used to conduct three-dimensional measurement of an air jet exhausted from a lobed nozzle. The characteristics of the mixing process in the lobed jet flow are revealed clearly and quantitatively from the stereoscopic PIV measurement results. The instantaneous velocity and streamwise vorticity distributions revealed that the large-scale streamwise vortices generated by the lobed nozzle break into smaller but not weaker streamwise vortices as they travel downstream. This is the proposed reason why a lobed nozzle would enhance both large-scale mixing and small-scale mixing reported by other researchers. The overall effect of the lobed nozzle on the mixing process was evaluated by analyzing the ensemble-averaged streamwise vorticity distributions. The strength of the ensemble-averaged streamwise vortices was found to decay very rapidly over the first two diameters (first six lobe heights), then to decay at a more moderate rate farther downstream. The averaged turbulent kinetic energy profile also indicated that most of the intensive mixing between the core jet and ambient flow occurred within the first two diameters. These results indicate that the maximum effectiveness region for the lobed nozzle to enhance mixing is about the first two diameters of the lobed nozzle (first six lobe heights).

Nomenclature

D	=	diameter of the lobed nozzle, 40 mm
H	=	lobe height, 15 mm
K	=	turbulent kinetic energy, $(1/2U_0^2)(u'^2 + v'^2 + w'^2)$
$\bar{K}(z)$	=	averaged-turbulent kinetic enegy, $\dfrac{\int \rho W(x, y, z) K(x, y, z)\, \mathrm{d}x\, \mathrm{d}y}{\int \rho W(x, y, z)\, \mathrm{d}x\, \mathrm{d}y}$
Re	=	Reynolds number
U, V, W	=	velocity three components
U_0	=	mean velocity of the air jet at the inlet of the lobed nozzle, 20.0 m/s
u', v', w'	=	rms values of velocity fluctuations
x, y, z	=	coordinates
θ_{in}	=	inward penetration angle of the lobed nozzle, 22 deg
θ_{out}	=	outward penetration angle of the lobed snozzle, 14 deg
μ	=	viscosity of air
ρ	=	density of air
ϖ_z	=	streamwise vorticity, $(D/U_0)(\partial v/\partial x - \partial u/\partial y)$

Introduction

LOBED mixers/nozzles, which are essentially splitter plates with corrugated trailing edges, are fluid mechanic devices used to augment mixing in a variety of applications. Such devices have been applied widely in turbofan engine exhausts and ejectors to reduce takeoff jet noise and specific fuel consumption.[1,2] More recently, lobed mixers/nozzles have also emerged as an attractive approach for enhancing mixing between fuel and air in combustion chambers to improve the efficiency of combustion and to reduce the formation of pollutants.[3]

Besides the continuous efforts to optimize the geometry of lobed mixers/nozzles for better mixing enhancement performance and widen the applications of lobed mixers/nozzles, extensive studies about the mechanism by which the lobed mixers/nozzles substantially enhance mixing have also been conducted in past years. Based on pressure, temperature, and velocity measurements of the flowfield downstream of a lobed nozzle, Paterson[4] revealed the existence of large-scale streamwise vortices in lobed mixing flows induced by the special geometry of lobed nozzles. The large-scale streamwise vortices were suggested to be responsible for the enhanced mixing. Werle et al.[5] and Eckerle et al.[6] found that the streamwise vortices in lobed mixing flows follow a three-step process by which the streamwise vortices form, intensify, and then break down and suggested that the high turbulence resulting from the vortex breakdown improved the overall mixing process. Elliott et al.[7] suggested that there are three primary contributors to the mixing processes in lobed mixing flows. The first is the spanwise vortices, which occur in any free shear layers due to the Kelvin–Helmholtz instability. The second is the increased interfacial contact area due to the convoluted trailing edge of the lobed mixer. The last element is the streamwise vortices produced by the special geometry of the lobed mixer. Based on pulsed laser sheet flow visualization with smoke and three-dimensional velocity measurements with a hot-film anemometer, McCormick and Bennett[8] suggested that it is the interaction of the spanwise Kelvin–Helmholtz vortices with the streamwise vortices that produce the high levels of mixing.

Although the existence of unsteady vortices and turbulent structures in lobed mixing flows has been revealed in those previous studies by qualitative flow visualization, the quantitative, instantaneous, whole-field velocity and vorticity distributions in lobed mixing flows have never been obtained until recent work of the present authors.[9] In Ref. 9, both planar laser induced fluorescence (PLIF) and conventional two-dimensional particle image velocimetry (PIV) techniques were used to study lobed jet mixing flows. Based on the directly perceived PLIF flow visualization images and quantitative PIV velocity, vorticity, and turbulence intensity distributions, the evolution and interaction of various vortical and turbulent structures in the lobed jet flows were discussed.

The conventional two-dimensional PIV system used in the earlier work of the authors[9] is only capable of obtaining two components

Received 27 February 2001; revision received 7 November 2001; accepted for publication 18 December 2001.

*Japan Society for the Promotion of Science Research Fellow, Institute of Industrial Science, 4-6-1 Komaba, Meguro-Ku; currently Postdoctoral Research Associate, Turbulent Mixing and Unsteady Aerodynamics Laboratory, A22, Research Complex Engineering, Michigan State University, East Lansing, MI 48824; huhui@egr.msu.edu. Member AIAA.

†Research Associate, Institute of Industrial Science, 4-6-1 Komaba, Meguro-Ku.

‡Professor, Institute of Industrial Science, 4-6-1 Komaba, Meguro-Ku.

§Associate Professor, Institute of Industrial Science, 4-6-1 Komaba, Meguro-Ku.

of velocity vectors in the planes of illuminating laser sheets. The out-of-plane velocity component is lost, whereas the in-plane components may be affected by an unrecoverable error due to perspective transformation.[10] For highly three-dimensional flows such as lobed jet mixing flows, conventional PIV measurement results may not be able to reveal their three-dimensional features successfully. A high-resolution stereoscopic PIV system, which can provide all three components of velocity vectors in a measurement plane simultaneously, is used in the present study to measure an air jet flow exhausted from a lobed nozzle. Based on the stereoscopic PIV measurement results, some characteristics of the mixing process in the lobed jet flow are discussed.

Experimental Setup and Stereoscopic PIV System

Figure 1a shows the lobed nozzle used in the present study. It has six lobe structures at the nozzle trailing edge. The width of each lobe is 6 mm, and the lobe height is 15 mm ($H = 15$ mm). The inward and outward penetration angles of the lobed structures are $\theta_{in} = 22$ deg and $\theta_{out} = 14$ deg, respectively. The diameter of the lobed nozzle is 40 mm ($D = 40$ mm).

Figure 1b shows the air jet experimental rig used in the present study. A centrifugal compressor was used to supply air jet flows. A cylindrical plenum chamber with honeycomb structures was used to settle the airflow. Through a convergent connection (convergent ratio 50:1), the airflow is exhausted from the lobed nozzle. The velocity range of the air jet out of the convergent connection (at the inlet of the test nozzle) could be varied from 5 to 35 m/s. A mean speed of the air jet flow at the inlet of the lobed nozzle of $U_0 = 20.0$ m/s was used, which corresponds to a Reynolds number $Re = 5.517 \times 10^5$ (based on the nozzle diameter $D = 40$ mm). The air jet flow was seeded with $1 \sim 5$-μm di-2-ethylhexyl-sebacat (DEHS) droplets generated by a seeding generator. The DEHS droplets out of the seeding generator were divided into two streams; one is used to seed the core jet flow and the other for ambient air seeding.

Figure 2 shows the schematic of the stereoscopic PIV system used. The lobed jet flow was illuminated by a double-pulsed Nd:YAG laser set (NewWave; 50-mJ/pulse) with the laser sheet thickness of about 2.0 mm. The double-pulsed Nd:YAG laser set can supply the pulsed laser (pulsed illumination duration 6 ns) at a frequency of 15 Hz. Two high-resolution (1000×1000) cross-correlation charge-coupled device (CCD) cameras (TSI PIVCAM10-30) were used to perform stereoscopic PIV image recording. The two CCD cameras were arranged in an angular displacement configuration to get a large overlapped view. With the installation of tilt-axis mounts, the lenses and camera bodies were adjusted to satisfy the Scheimpflug condition (see Ref. 11). In the present study, the distance between the illuminating laser sheet and image recording planes of the CCD cameras is about 650 mm, and the angle between the view axis of the two cameras is about 50 deg. For such an arrangement, the size of the stereoscopic PIV measurement window is about 80×80 mm^2.

The CCD cameras and double-pulsed Nd:YAG lasers were connected to a workstation (host computer) via a synchronizer (TSI LaserPulse synchronizer), which controlled the timing of the laser sheet illumination and the CCD camera data acquisition. In the present study, the time interval between the two pulsed illuminations is 30 μs.

A general in situ calibration procedure was conducted to obtain the mapping functions between the image planes and object planes.[12] A target plate (100×100 mm) with 100-μm-diam dots spaced at intervals of 2.5 mm was used for the in situ calibration. The front surface of the target plate was aligned with the center of the laser sheet, and then calibration images were captured at three locations across the depth of the laser sheets. The space interval between these locations is 0.5 mm for the present study.

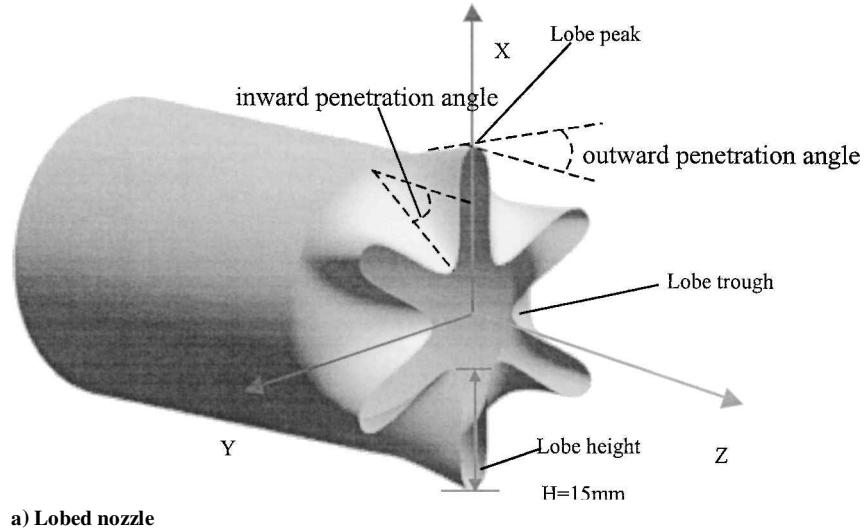

a) Lobed nozzle

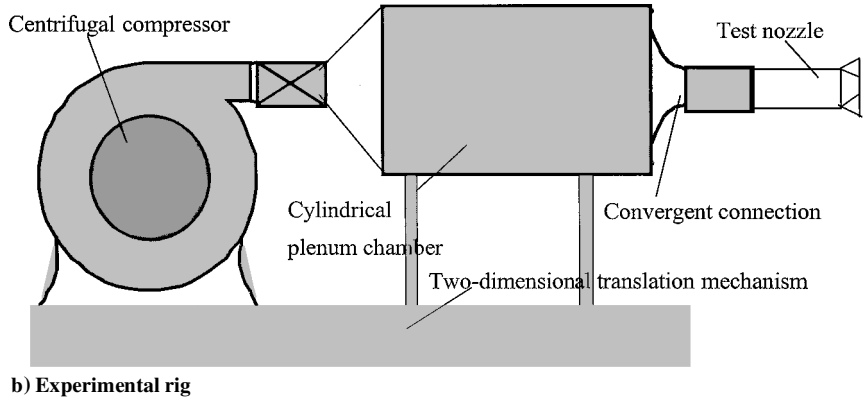

b) Experimental rig

Fig. 1 Lobed nozzle and air jet experimental rig.

The mapping function used was taken to be a multidimensional polynomial, which is fourth order for the directions (X and Y directions) parallel to the laser sheet plane and second order for the direction (Z direction) normal to the laser sheet plane. The coefficients of the multidimensional polynomial were determined from the calibration images by using a least-square method.

The two-dimensional particle image displacements in each image plane was calculated separately by using a hierarchical recursive PIV (HR-PIV) software developed in-house. The HR-PIV software is based on HR processes of a conventional spatial correlation operation with offsetting of the displacement estimated by the former iteration step and hierarchical reduction of the interrogation window size and search distance in the next iteration step.[13] Compared with conventional cross-correlation-based PIV image processing methods, the HR-PIV method has advantages in spurious vector suppression and spatial resolution improvement of the PIV result. Finally,

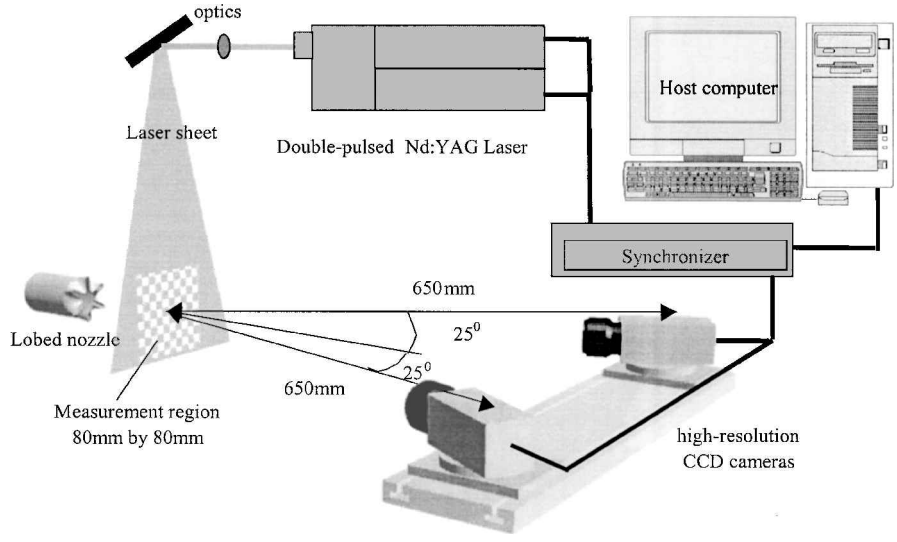

Fig. 2 Stereoscopic PIV system.

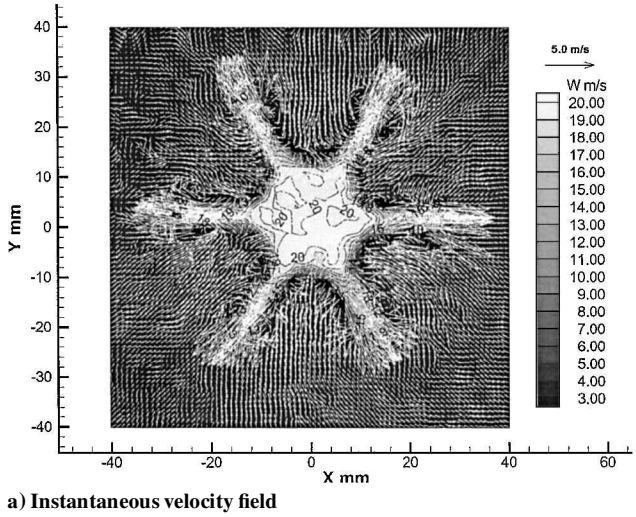

a) Instantaneous velocity field

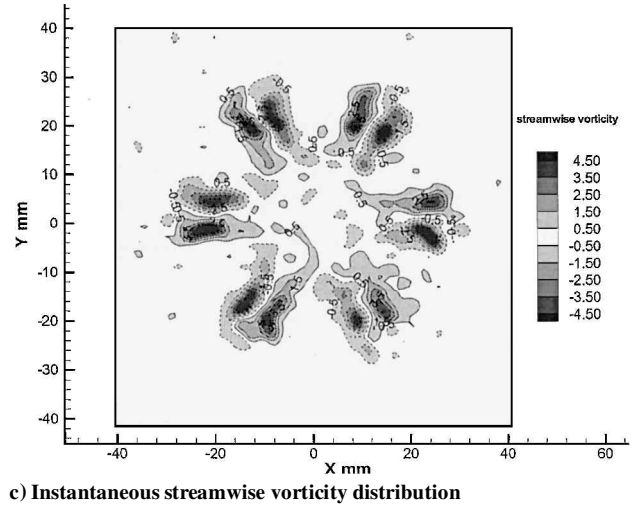

c) Instantaneous streamwise vorticity distribution

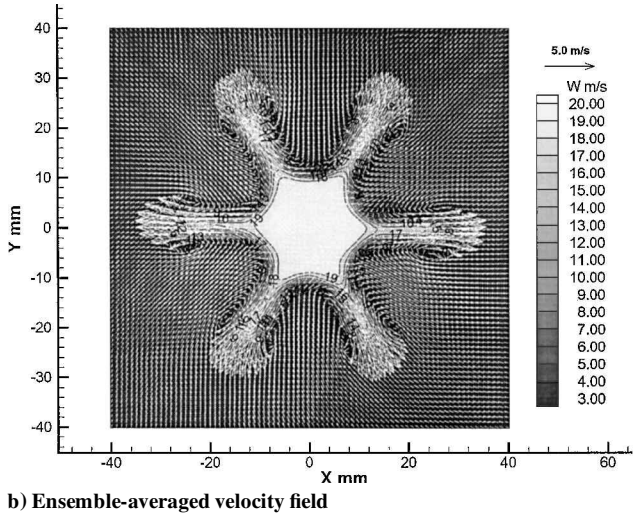

b) Ensemble-averaged velocity field

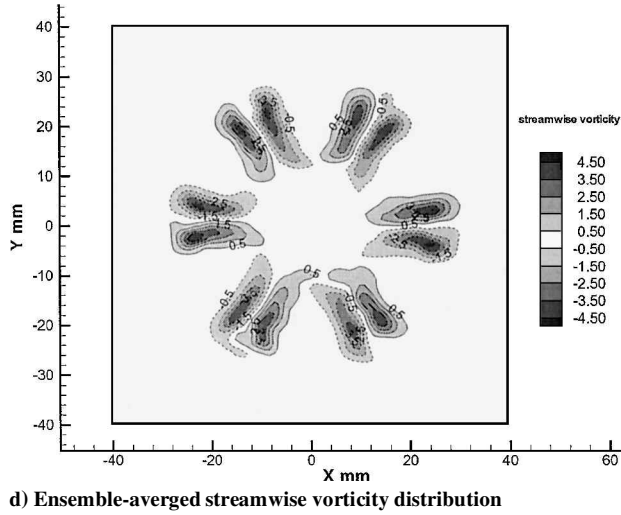

d) Ensemble-averged streamwise vorticity distribution

Fig. 3 Stereoscopic PIV measurement results in the $Z/D = 0.25$ ($Z/H = 0.67$) cross plane.

when the mapping functions obtained by the in situ calibration and the two-dimensional displacements in the two image planes are used, all three components of the velocity vectors in the illuminating laser sheet plane were reconstructed.

Because 32 × 32 pixel interrogation windows with 50% overlap were used for the final step of the recursive correlation operation, the spatial resolution of the present stereoscopic PIV measurement is expected to be about $2.5 \times 2.5 \times 2.0$ mm^3. To evaluate the measurement accuracy of the present stereoscopic PIV system, a laser doppler velocimetry (LDV) system was used to conduct simultaneous measurement of the lobed jet flow. The stereoscopic PIV measurement results were compared with the LDV results. It was found that the velocity differences between the measurement results of the stereoscopic PIV system and the LDV data are less than 2.0% at the compared points. Therefore, the accuracy level of the velocity vectors obtained by the stereoscopic PIV system is expected to be about 2.0% and that of the rms of the velocity fluctuations, u', v', and w', and turbulent kinetics energy K are about 5.0%. An adaptive scheme[14] was used in the present study to calculate streamwise vorticity ϖ_z distributions from the velocity fields obtained by the stereoscopic PIV measurement. The accuracy level of the streamwise vorticity data in the present study is expected to be within 10.0%. Further details about the in situ calibration, reconstruction procedures of the stereoscopic PIV system and the comparison of the stereoscopic PIV and LDV measurements may be found in Ref. 15.

Experimental Results and Discussion

Figures 3–5 shows the stereoscopic PIV measurement results in three typical cross planes of the lobed jet flow, which include typical instantaneous velocity fields, simultaneous streamwise vorticity distributions, ensemble-averaged velocity, and streamwise vorticity fields. The ensemble-averaged velocity and streamwise vorticity fields given in Figs. 3–5 were calculated based on 250 frames of instantaneous stereoscopic PIV measurement results.

In the $Z/D = 0.25$ ($Z/H = 0.67$) cross plane (almost at the exit of the lobed nozzle), the high-speed core jet flow was found to have the same geometry as the lobed nozzle. The signature of the lobed nozzle in the form of a six-lobe structure can be seen clearly from both the instantaneous and ensemble-averaged velocity fields (Fig. 3). The existence of very strong secondary streams in the lobed jet flow is revealed very clearly in the velocity vector plots. The core jet flow ejects radially outward in the lobe peaks, and ambient flows inject inward in the lobe troughs. Both the ejection of the core jet flow and the injection of the ambient flows generally are following the outward and inward contours of the lobed nozzle, which results in the generation of six pairs of counterrotating streamwise vortices in the lobed jet flow. The maximum radial ejection velocity of the core jet flow in the ensemble-averaged velocity field is found to be about 5.0 m/s, which is almost equal to the value of $U_0 \cdot \sin(\theta_{out})$. A large high-speed region can also be seen clearly from the ensemble-averaged velocity field, which represents the high-speed core jet flow in the center of the lobed nozzle.

The existence of the six pairs of large-scale streamwise vortices due to the special geometry of the lobed nozzle can be seen more clearly and quantitatively from the streamwise vorticity distributions shown in Figs. 3c and 3d. The size of these large-scale streamwise vortices is found to be on the order of the lobe height. Compared with those in the instantaneous streamwise vorticity field (Fig. 3c), the contours of the large-scale streamwise vortices in the ensemble-averaged streamwise vorticity field (Fig. 3d) were found

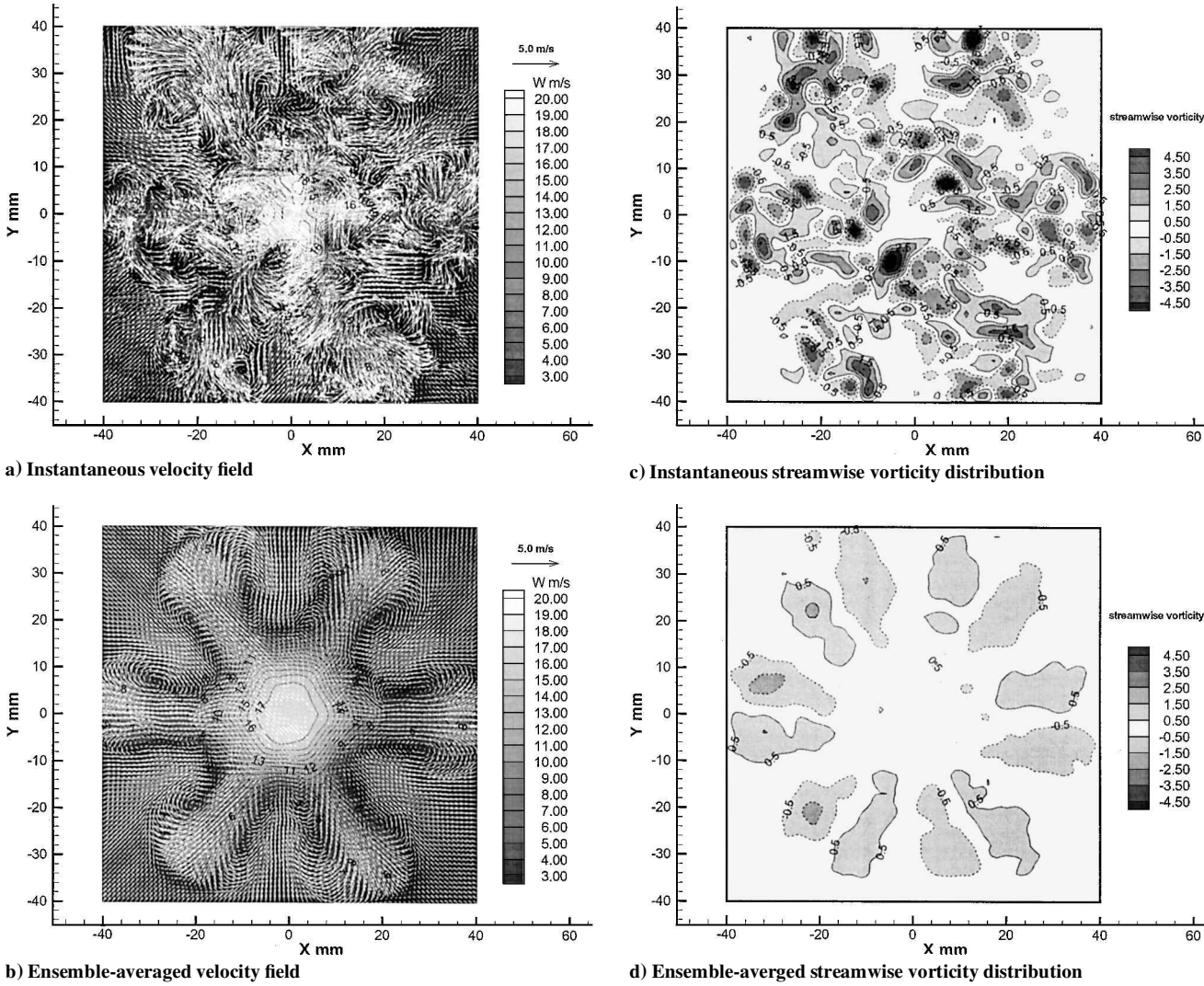

a) Instantaneous velocity field

c) Instantaneous streamwise vorticity distribution

b) Ensemble-averaged velocity field

d) Ensemble-averged streamwise vorticity distribution

Fig. 4 Stereoscopic PIV measurement results in the $Z/D = 1.5$ ($Z/H = 4.0$) cross plane.

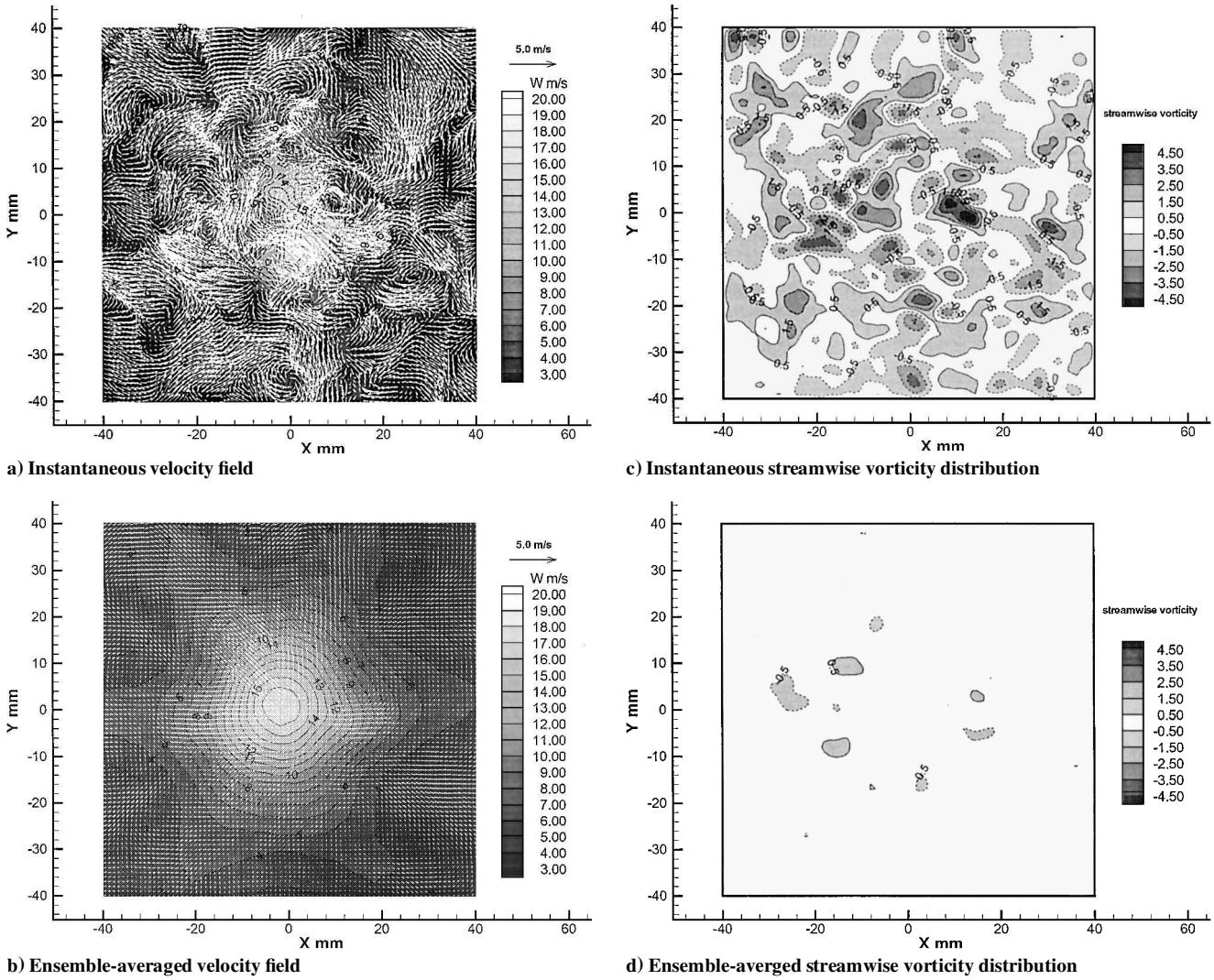

a) Instantaneous velocity field

c) Instantaneous streamwise vorticity distribution

b) Ensemble-averaged velocity field

d) Ensemble-averged streamwise vorticity distribution

Fig. 5 Stereoscopic PIV measurement results in the $Z/D = 3.0$ ($Z/H = 8.0$) cross plane.

to be much smoother. However, they have almost the same distribution pattern and magnitude as their instantaneous counterparts. The similarities between the instantaneous and ensemble-averaged streamwise vortices might suggest that the generation of large-scale streamwise vortices at the exit of the lobed nozzle to be quite steady.

The lobed jet flow was found to become much more turbulent in the $Z/D = 1.5$ ($Z/H = 6.0$) cross plane compared to that at the exit of the lobed nozzle. Instead of generally following the inward and outward contours of the lobed trailing edge at the exit of the lobed nozzle, the secondary streams revealed in the instantaneous velocity field (Fig. 4a) become much more random and unsteady. The signature of the lobed nozzle in the form of a six-lobe structure is nearly indistinguishable from the instantaneous velocity field. Although the high-speed region in the center of the lobed nozzle still can be discerned from the ensemble-averaged velocity field, the size of the high-speed region was found to decrease substantially due to intensive mixing between the core jet flow and ambient flow. The ensemble-averaged velocity vector plot also shows that the ensemble-averaged secondary streams in the lobed jet flow have become much weaker. The maximum radial ejection velocity of the core jet flow has decreased to about 2.0 m/s, which is only about 40% of that at the exit of the lobed nozzle.

The six pairs of large-scale streamwise vortices generated by the lobed nozzle could no longer be identified from the instantaneous streamwise vorticity distribution in the $Z/D = 1.5$ ($Z/H = 4.0$) cross plane shown in Fig. 4c. Instead of large-scale streamwise vortices, many smaller streamwise vortices were found in the instantaneous streamwise vorticity field. This indicates that the large-scale streamwise vortices observed at the exit of the lobed nozzle have broken down into many smaller streamwise vortices. However, note that the maximum vorticity value of the instantaneous small-scale streamwise vortices is found to be almost at the same level as those at the exit of the lobed nozzle.

From the ensemble-averaged streamwise vorticity distribution in this cross plane (Fig. 4d), note that the strength of the large-scale ensemble-averaged streamwise vortices in the lobed jet flow has dissipated. The maximum value of the ensemble-averaged streamwise vorticity is only about one-fifth of that at the exit of the lobed nozzle. Because the present lobed jet flow is a freejet, the centers of the large-scale streamwise vortices were found to have spread outward as they travel downstream, which is also revealed very clearly in the ensemble-averaged velocity vector plot given in Fig. 4b. The same phenomena were also found in the LDV measurement results of Belovich and Samimy.[16]

As the downstream distance increases to $Z/D = 3.0$ ($Z/H = 8.0$), the lobed jet mixing flow became so turbulent that the signature of the lobed nozzle can no longer be identified from the instantaneous velocity field (Fig. 5a). The flowfield is completely filled with many small-scale vortices and turbulent structures. The ensemble-averaged velocity field in this cross plane shows that the distinct high-speed region in the center of the lobed jet flow has dissipated so seriously that isovelocity contours of the high-speed core jet flow have become small concentric circles. The ensemble-averaged secondary streams in this cross plane become so weak (the maximum secondary stream velocity of less than 0.8 m/s) that they can not be identified easily from the ensemble-averaged velocity vector plot.

From the instantaneous streamwise vorticity distribution in the $Z/D = 3.0$ ($Z/H = 8.0$) cross plane given in Fig. 5c, note that there are so many small-scale streamwise vortices in the lobed jet mixing flow that they almost filled the measurement window. However, the maximum vorticity value of these instantaneous small-scale streamwise vortices was found to be still at the same level of those in the upstream cross planes. Because of serious dissipation caused by the intensive mixing between the core jet flow and ambient flow, almost no apparent streamwise vortices can be identified from the ensemble-averaged streamwise vorticty distribution (Fig. 5d) in the $Z/D = 3.0$ ($Z/H = 6.0$) cross plane.

Based on the stereoscopic PIV measurement results at 12 cross planes, the ensemble-averaged three-dimensional flowfield in the near downstream region of the lobed jet flow was reconstructed. Figure 6a shows the three-dimensional ensemble-averaged velocity vectors. The velocity isosurfaces of the reconstructed three-dimensional flowfield are given in Fig. 6b. The velocity magnitudes of these isosurfaces are 4.0, 8.0, 12.0, and 16.0 m/s, respectively. Note that the high-speed core jet flow has the same geometry as the lobed nozzle, that is, six-lobe structure, at the exit of the lobed nozzle. Because of the stirring effect of the large-scale streamwise vortices generated by the lobed nozzle, the six-lobe structure of the core jet flow was rounded up rapidly. At $Z/D = 3.0$ ($Z/H = 8.0$) downstream, the isosurfaces were found to become concentric cylinders, which are very similar to those in a circular jet flow.

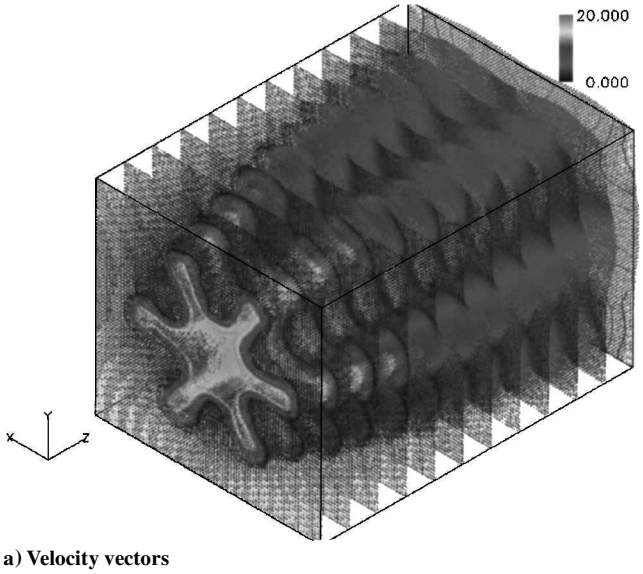

a) Velocity vectors

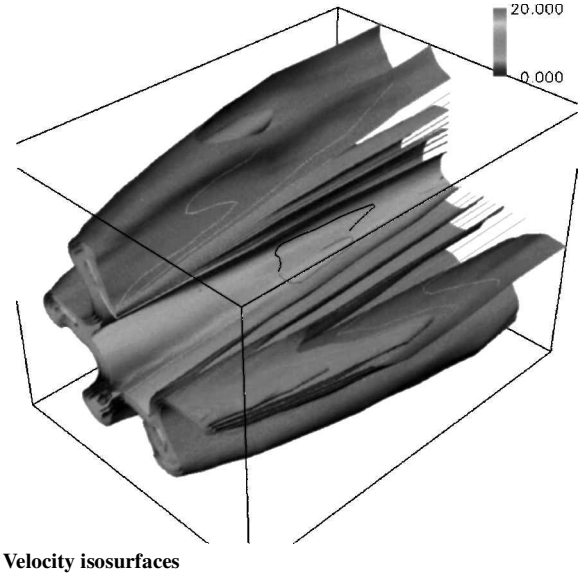

b) Velocity isosurfaces

Fig. 6 Reconstructed three-dimensional flowfield.

The preceding stereoscopic PIV measurement results have shown that the size of the instantaneous streamwise vortices in the lobed jet flow decreases as the downstream distance increases, that is, the large-scale streamwise vortices generated by the lobed nozzle broke into smaller vortices as they travel downstream. However, the maximum vorticity values of the smaller vortices were found to be almost at the same level as their parent streamwise vortices. These results suggested that the dissipation of the large-scale streamwise vortices generated by the corrugated trailing edge of the lobed nozzle did not happen abruptly but rather appeared to be a gradual process. The large streamwise vortices were found to break down into many smaller but not weaker streamwise vortices as the downstream distance increases. Thus, besides the large-scale mixing enhancement, mixing at a finer scale could also be achieved in the lobed jet mixing flow. The result, therefore, agrees well with those obtained by Belovich et al.[17]

The lobed nozzle might be thought to act as a fluid stirrer in the lobed jet flow to mix the core jet flow with ambient flow. The stirring effect of the lobed nozzle on the mixing processes can be evaluated from the evolution of the ensemble-averaged streamwise vortices. Figure 7 shows the decay profile of the ensemble-averaged streamwise vorticity in the lobed jet flow. Note that, over the first two diameters downstream of the lobed nozzle (first six lobe heights), the ensemble-averaged streamwise vorticity decayed very rapidly and then the decay rate slowed farther downstream. This may indicate that the stirring effect of the lobed nozzle to enhance the mixing between the core jet flow and ambient flow is concentrated primarily in the first two diameters (first six lobe heights). In the cross plane of $Z/D = 3.0$ ($Z/H = 8.0$), the ensemble-averaged streamwise vorticity dissipated so seriously that the strength of the ensemble-averaged streamwise vortices became only about $\frac{1}{10}$th of that at the exit of the lobed nozzle. This means that the stirring effect of the lobed nozzle has almost disappeared at this downstream location.

The characteristics of the mixing process between the core jet flow and ambient flow in the lobed jet flow may be revealed more quantitatively from the averaged-turbulent kinetic energy profile given in Fig. 8. In the present paper, the averaged-turbulent kinetic energy

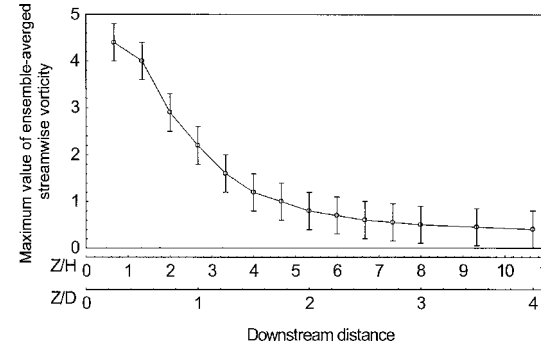

Fig. 7 Decay of the ensemble-averaged streamwise vorticity.

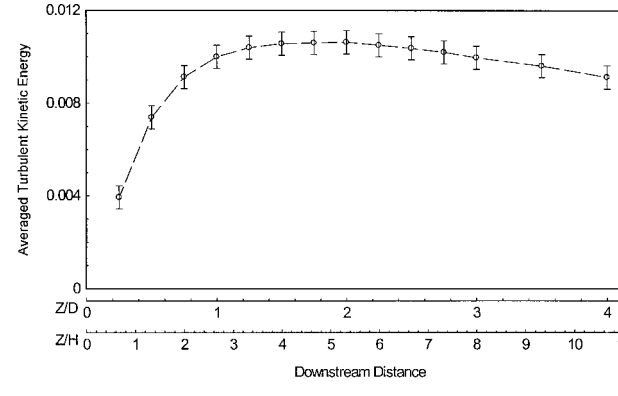

Fig. 8 Averaged turbulent kinetic energy profile.

of the lobed jet flow at each measured cross plane was calculated by using the following equation:

$$\bar{K}(z) = \frac{\int \rho W(x, y, z) K(x, y, z)\, dx\, dy}{\int \rho W(x, y, z)\, dx\, dy}$$

It was found that the averaged-turbulentkinetic energy grew very rapidly within the first diameter of the lobed nozzle and then decreased to a more moderate rate farther downstream. The averaged-turbulent kinetic energy profile reached its peak value at about $Z/D = 2.0$ ($Z/H = 5.33$) and then began to decrease. This may be explained as follows. Within the first one diameter of the test nozzle, due to the stirring effect of the large-scale streamwise vortices generated by the lobed nozzle revealed in the given streamwise vorticity distributions, the core jet flow and ambient flow mixed intensively. In the downstream region of $Z/D > 1.0$ ($Z/H > 2.67$), the large-scale streamwise vortices generated by the lobed nozzle were found to break down into smaller vortices, that is, the stirring effect of the large-scale streamwise vortices weakened. Thus, the growth rate of the averaged turbulent kinetic energy was found to decrease and to reach its peak at about $Z/D = 2.0$ ($Z/H = 5.33$). The ensemble-averaged streamwise vorticity has become so weak that it almost cannot affect the mixing process in the farther downstream region. Because most of the turbulent kinetic energy in the lobed jet mixing flow dissipated in the intensive mixing upstream, the averaged turbulent kinetic energy begins to decrease. It may also indicate that most of the enhancement of mixing caused by the lobe nozzle occurs within the first two diameters. This result is also found to agree with the findings of McCormick and Bennett[8] and Glauser et al.[18] in a planar lobed mixing flow, who suggested that the maximum effectiveness region for a lobed mixer is about the first six lobe heights.

Because large-scale streamwise vortices generated by the lobed nozzle were dissipated in the farther downstream region ($Z/D > 3.0$, $Z/H > 8.0$), they no longer can enhance the mixing process in the lobed jet flow. The ensemble-averaged velocity distributions and velocity isosurfaces shown in Figs. 5 and 6 reveal that the isovelocity contours in the lobed jet flow in the farther downstream region ($Z/D > 3.0$, $Z/H > 8.0$) become concentric circles, which are similar to those in a circular jet flow. Therefore, the mixing between the core jet flow and the ambient flow in the farther downstream region ($Z/D > 3.0$, $Z/D > 8.0$) is expected to occur by the same gradient-type mechanism as that in a conventional circular jet flow.

Summary

A high-resolution stereoscopic PIV system was used to measure an air jet flow exhausted from a lobed nozzle. The evolution of the large-scale streamwise vortices in the lobed jet flow, which originated from the strong secondary streams due to the geometry of the lobed trailing edge, was revealed instantaneously and quantitatively from the stereoscopic PIV measurement results. The instantaneous velocity fields reveal that the core jet flow expands radially outward in the lobe peaks and ambient flow injects inward in the lobe troughs at the exit of the lobed nozzle, which results in the generation of large-scale, counter-rotating streamwise vortices in the lobed jet flow. The large-scale streamwise vortices break down into smaller but not weaker vortices as they travel downstream. This is proposed as the reason that a lobed nozzle would enhance both large-scale mixing and small-scale mixing reported by other researchers. The overall effect of the lobed nozzle on the mixing process in the lobed jet flow was evaluated by analyzing the evolution of the ensemble-averaged streamwise vorticity distributions. The strength of the ensemble-averaged streamwise vortices was found to decay very rapidly in the first two diameters of the lobed nozzle, then turn to a moderate decay rate farther downstream. This may indicate that the stirring effect of the lobed nozzle to enhance mixing between the core jet flow and ambient flow is concentrated primarily in the first two diameters of the lobed nozzle (first six lobe heights). The averaged turbulent kinetic energy profile also indicated that most of the intensive mixing between the core jet flow and ambient flow occurred over the first two diameters of the lobed jet flow (first six lobe heights). The isovelocity contours of the lobed jet flow in the farther downstream regions ($Z/D > 3.0$, $Z/H > 12.0$) are found to be concentric circles, which are quite similar as those in a circular jet flow. These results indicate that the mixing enhancement caused by the special geometry of the lobed nozzle concentrates primarily in the first two diameters downstream of the lobed nozzle (first six lobe heights). The mixing between the core jet flow and ambient flow in the farther downstream region ($Z/D > 3.0$, $Z/H > 12.0$) will occur by the same gradient-type mechanism as that for a circular jet flow.

References

[1]Kuchar, A. P., and Chamberlin, R., "Scale Model Performance Test Investigation of Exhaust System Mixers for an Energy Efficient Engine (E^3)," AIAA Paper 80-0229, 1980.

[2]Presz, W. M., Jr., Reynolds, G., and McCormick, D., "Thrust Augmentation Using Mixer–Ejector–Diffuser Systems," AIAA Paper 94-0020, 1994.

[3]Smith, L. L., Majamak, A. J., Lam, I. T., Delabroy, O., Karagozian, A. R., Marble, F. E., and Smith, O. I., "Mixing Enhancement in a Lobed Injector," *Physics of Fluids*, Vol. 9, No. 3, 1997, pp. 667–678.

[4]Paterson, R. W., "Turbofan Forced Mixer Nozzle Internal Flowfield," NASA CR-3492, 1982.

[5]Werle, M. J., Paterson, R. W., and Presz, W. M., Jr., "Flow Structure in a Periodic Axial Vortex Array," AIAA Paper 87-6l0, 1987.

[6]Eckerle, W. A., Sheibani, H., and Awad, J., "Experimental Measurement of the Vortex Development Downstream of a Lobed Forced Mixer," *Journal of Engineering for Gas Turbine and Power*, Vol. 114, Jan. 1992, pp. 63–71.

[7]Elliott, J. K., Manning, T. A., Qiu, Y. J., Greitzer, C. S., Tan, C. S., and Tillman, T. G., "Computational and Experimental Studies of Flow in Multi-Lobed Forced Mixers," AIAA Paper 92-3568, 1992.

[8]McCormick, D. C., and Bennett, J. C., Jr., "Vortical and Turbulent Structure of a Lobed Mixer Free Shear Layer," *AIAA Journal*, Vol. 32, No. 9, 1994, pp. 1852–1859.

[9]Hu, H., Saga, T., Kobayashi, T., and Taniguchi, N., "Research on the Vortical and Turbulent Structures in the Lobed Jet Flow by Using LIF and PIV," *Measurement Science and Technology*, Vol. 11, No. 6, 2000, pp. 698–711.

[10]Prasad, A. K., and Adrian, R. J., "Stereoscopic Particle Image Velocimetry Applied to Fluid Flows," *Experiments in Fluids*, Vol. 15, No. 1, 1993, pp. 49–60.

[11]Prasad, A. K., and Jensen, K., "Scheimpflug Stereocamera for Particle Image Velocimetry in Liquid Flows," *Applied Optics*, Vol. 34, No. 30, 1995, pp. 7092–7099.

[12]Soloff, S. M., Adrian, R. J., and Liu, Z. C., "Distortion Compensation for Generalized Stereoscopic Particle Image Velocimetry," *Measurement Science and Technology*, Vol. 8, No. 12, 1997, pp. 1441–1454.

[13]Hu, H., Saga, T., Kobayashi, T., Taniguchi, N., and Segawa, S., "Improve the Spatial Resolution of PIV Results by Using Hierarchical Recursive Operation," *Proceedings of 9th International Symposium on Flow Visualization*, edited by G. M. Carlomagno and I. Grant, Paper 137, 2000.

[14]Lourenco, L., and Krothapalli, A., "On the Accuracy of Velocity and Vorticity Measurements with PIV," *Experiments in Fluids*, Vol. 18, No. 6, 1995, pp. 421–428.

[15]Hu, H., "Investigation on Lobed Jet Mixing Flows by Using PIV and LIF Techniques," Ph.D. Dissertation, Dept. of Mechanical Engineering, Univ. of Tokyo, Tokyo, April 2001.

[16]Belovich, V. M., and Samimy, M., "Mixing Process in a Coaxial Geometry with a Central Lobed Mixing Nozzle," *AIAA Journal*, Vol. 35, No. 5, 1997, pp. 838–84l.

[17]Belovich, V. M., Samimy, M., and Reeder, M. F., "Dual Stream Axisymmetric Mixing in the Presence of Axial Vorticity," *Journal of Propulsion and Power*, Vol. 12, No. 1, 1996, pp. 178–185.

[18]Glauser, M., Ukeiley, L., and Wick, D., "Investigation of Turbulent Flows Via Pseudo Flow Visualization, Part 2: The Lobed Mixer Flow Field," *Experimental Thermal and Fluid Science*, Vol. 13, No. 2, 1996, pp. 167–177.

J. P. Gore
Associate Editor